Published online 13 September 2013 *Nucleic Acids Research, 2013, Vol. 41, No. 22* ***10323–10333***
doi:10.1093/nar/gkt813

DNA polymerase δ stalls on telomeric lagging strand templates independently from G-quadruplex formation

Justin D. Lormand[1], Noah Buncher[1], Connor T. Murphy[1], Parminder Kaur[2], Marietta Y. Lee[3], Peter Burgers[4], Hong Wang[2], Thomas A. Kunkel[5] and Patricia L. Opresko[1,*]

[1]Department of Environmental and Occupational Health, University of Pittsburgh Graduate School of Public Health, 100 Technology Drive, Pittsburgh, PA 15219, USA, [2]Department of Physics, North Carolina State University, 2401 Stinson Drive, Raleigh, NC, 27695, USA, [3]Department of Biochemistry and Molecular Biology, New York Medical College, Valhalla, NY 10595, USA, [4]Department of Biochemistry and Molecular Biophysics, Washington University School of Medicine, St. Louis, MO 63110, USA and [5]Laboratory of Molecular Genetics and Laboratory of Structural Biology, National Institute of Environmental Health Sciences, NIH, DHHS, Research Triangle Park, NC 27709, USA

Received May 14, 2013; Revised August 16, 2013; Accepted August 19, 2013

ABSTRACT

Previous evidence indicates that telomeres resemble common fragile sites and present a challenge for DNA replication. The precise impediments to replication fork progression at telomeric TTAGGG repeats are unknown, but are proposed to include G-quadruplexes (G4) on the G-rich strand. Here we examined DNA synthesis and progression by the replicative DNA polymerase δ/proliferating cell nuclear antigen/replication factor C complex on telomeric templates that mimic the leading C-rich and lagging G-rich strands. Increased polymerase stalling occurred on the G-rich template, compared with the C-rich and nontelomeric templates. Suppression of G4 formation by substituting Li^+ for K^+ as the cation, or by using templates with 7-deaza-G residues, did not alleviate Pol δ pause sites within the G residues. Furthermore, we provide evidence that G4 folding is less stable on single-stranded circular TTAGGG templates where ends are constrained, compared with linear oligonucleotides. Artificially stabilizing G4 structures on the circular templates with the G4 ligand BRACO-19 inhibited Pol δ progression into the G-rich repeats. Similar results were obtained for yeast and human Pol δ complexes. Our data indicate that G4 formation is not required for polymerase stalling on telomeric lagging strands and suggest that an alternative mechanism, in addition to stable G4s, contributes to replication stalling at telomeres.

INTRODUCTION

Telomeres are nucleoprotein structures that prevent degradation at chromosomes ends and chromosome end-to-end fusions. Human telomeres consist of linear arrays of 5–10 kb of TTAGGG repeats and end in a 3′ single-strand overhang. These repeats are necessary binding sites for the shelterin protein complex, which isolates telomeres from the DNA damage surveillance machinery (1). Loss of telomeric DNA or shelterin proteins cause chromosome ends to be recognized as DNA double-strand breaks, which leads to growth arrest or chromosome alterations (2). Telomeres shorten with each cell division owing to the inability to completely replicate chromosome ends (3), which is compensated for by telomerase. However, most human somatic cells lack telomerase activity and the majority of the telomere is maintained through semiconservative DNA replication during cell division (4). Therefore, maintaining replication fork progression through repetitive telomeric templates is critical for preserving chromosome ends and overall genome stability.

Emerging data reveal that telomeres resemble common fragile site sequences in the genome because they are prone to alterations or breakage under replication stress conditions (5–7). The inhibition of replicative DNA polymerases or defects in replication stress checkpoints, generates breaks at common fragile site sequences and causes

*To whom correspondence should be addressed. Tel: +1 412 624 8285; Fax: +1 412 624 9361; Email: plo4@pitt.edu

telomere doublets at chromosome ends that resemble fragmented telomeres (5,8). Defects in telomere replication can also yield chromatid ends that lack a telomere signal, presumably owing to telomere loss caused by failures in telomere replication (9,10). Therefore, telomeres and fragile site sequences share the common feature of being challenging to replicate.

The precise obstacles to telomere replication are not well defined. However, evidence from yeast and mammalian cells indicate that shelterin proteins suppress fork stalling during telomere replication (5,8). Shelterin proteins can recruit specialized DNA helicases including Bloom Syndrome helicase (BLM), RTEL and Werner syndrome helicase (WRN) to the telomeres, and these helicases also suppress telomere fragility or stochastic telomere loss, which suggests that secondary DNA structures impede replication (5,9,11–13). Tandem TTAGGG single-stranded repeats can fold into G-quadruplex (G4) DNA, which are four-stranded DNA structures that are stabilized via Hoogsteen base pairing between guanines (14). Because telomeres lack a known origin of replication, the G-rich template is replicated by lagging strand DNA synthesis and may fold into G4 DNA in the single-stranded DNA (ssDNA) gaps of Okazaki fragments. WRN is required to prevent the loss of telomeres replicated from the G-rich lagging strand in human cells (9,15), and many helicases can unwind G4 structure *in vitro* (16,17). Bimolecular G4 folds in the (CGG)n sequence were shown to block DNA polymerase δ (Pol δ) progression (18), which is the enzyme primarily responsible for replicating the lagging strand template (19). Collectively, these data led to the model that replication forks stall at telomeres owing to the propensity for G4 folding, and that specialized DNA helicases promote telomere replication by unwinding G4 DNA (5,20–22). However, other potential obstacles exist at telomeres (23), and DNA synthesis by Pol δ on lagging or leading strand telomeric templates had not been examined.

Here we directly tested the model that Pol δ stalls during DNA synthesis on telomeric lagging strand DNA templates owing to G4 folding. Consistent with previous predictions, we observed that Pol δ pauses at the G runs within TTAGGG repeats, even in the presence of the proliferating cell nuclear antigen (PCNA) processivity clamp and replication factor C (RFC) clamp loader. Surprisingly, stalling is still observed even under conditions that suppress G4 folding. Our data indicate that besides G4 formation, other mechanisms, such as specific sequence context effects, may contribute to telomere fragility during DNA replication.

MATERIALS AND METHODS

Protein purification

Recombinant yeast Pol δ was purified as described (24), and recombinant yeast PCNA and RFC were purified from *Escherichia coli* overproduction strains as described (25). Recombinant 4 subunit, human Pol δ and PCNA were purified as previously described (26). Recombinant human replication protein A was kindly provided by Dr Walter Chazin. Recombinant protection of telomeres 1 (POT1) protein was purified using a baculovirus/insect cell expression system and an AKTA Explorer FPLC (GE Health Care, Piscataway, NJ, USA) as described previously (27).

DNA substrates

Oligonucleotides were purchased from Integrated DNA Technologies and were purified using polyacrylamide gel electrophoresis by the manufacturer. The oligonucleotide with two 7-deazaguanine residues was purchased from Midland Certified Reagents Company. The sequences of the various primers are indicated in Supplementary Table S1. Primers were 5′-end-labeled with [γ-^{32}P]ATP (3000 Ci/mmol) (PerkinElmer Life Sciences) using Optikinase (Affymetrix), according to the manufacturer's protocol. The telomeric sequences were inserted into pGTK4 vector, which is a derivative of pGEM3zf(−) (Promega Corporation) as described (28). Log-phase cultures of plasmid-bearing *E. coli* strain DH5αIQ were infected with R408 helper phage for 3 h for the generation of ssDNA, which was purified as described (29). Primers were annealed to ssDNA vectors in 0.4× saline-sodium citrate, which equates to 60 mM NaCl, unless otherwise indicated in the figure legend. Linear oligonucleotide templates were prepared by annealing primers in either 100 mM KCl or 100 mM LiCl.

Atomic force microscopy analysis of G4 formation

Circular duplex DNA substrates containing a 157-nt region of ssDNA were prepared as described previously (30). The ssDNA region contained either $(TTAGGG)_{10}$ or $CCTAA(CCCTAA)_9C$ sequences flanked by 28 5′ and 69 3′ nucleotides. The linear $(TTAGGG)_{10}$ DNA molecules were constructed by annealing the Tel10 oligonucleotide with the 6-nt running start (RS) primer (Supplementary Table S1). DNA substrates were diluted to a final concentration of 1 μg/ml in a buffer containing 25 mM Hepes, pH 7.5, 25 mM Na-acetate and 10 mM $MgCl_2$ and deposited onto a freshly cleaved mica surface (SPI Supply). All samples were washed with MilliQ water and dried under a stream of nitrogen gas. Images were collected in tapping mode using a MultiModeV microscope (Bruker Corporation) with an E scanner or a MFP-3D-BIO atomic force microscopy (AFM; Asylum Research). PPP-NCL or PPP-FMR AFM probes (Nanosensors) were used. Images were captured at a scan size of 1–4 μm^2, a scan rate of 1–2 Hz and a resolution of 512 × 512 pixels.

DNA polymerase reactions

Standard reactions for yeast Pol δ contained 20 mM Tris, pH 7.8, 0.2 mg/ml bovine serum albumin, 1 mM dithiothreitol (DTT), 90 mM NaCl (unless otherwise indicated), 10 mM magnesium acetate, 100 μM deoxynucleotide (dNTP), 0.5 mM ATP and 6.6 nM DNA substrate. Where indicated in the figure legend, the DNA substrate was preincubated with 20 nM PCNA and 13 nM RFC for 5 min at 30°C, and the reactions were initiated by adding Pol δ. Standard reactions for human

Pol δ contained 40 mM Tris, pH 7.8, 0.2 mg/ml bovine serum albumin, 1 mM DTT, 5 mM NaCl (unless otherwise indicated), 10 mM $MgCl_2$, 0.5 mM ATP, 250 μM dNTP and 6.6 nM DNA substrate. Where indicated in the figure legend, the DNA substrate was preincubated with 170 nM human PCNA and 13 nM RFC for 5 min at 37°C, and the reactions were then initiated by adding Pol δ. At the specified time points, 8 μl aliquots were removed from the reactions and terminated using 95% formamide and 5 mM EDTA. Reaction products were resolved on a 10% denaturing polyacrylamide gel and visualized with a Typhoon 9400 phosphoimager. Products and unused primer were quantitated by ImageQuant software and were corrected for background in the no enzyme control reactions. The percent of primer degradation was calculated as the amount of radioactivity in bands for shortened primers divided by total radioactivity in the lane. To analyze the extent of DNA synthesis, the amount of radioactivity in bands for products terminated before the telomeric sequence (RS) or for products terminated within and beyond (5′) the telomeric sequence, was divided by the total amount of radioactivity in the lane.

RESULTS

Pol δ DNA synthesis on telomeric templates

We first examined telomeric lagging strand DNA synthesis by Pol δ from *Saccharomyces cerevisiae*. Although the telomeric sequence in budding yeast differs from human, the telomere lagging strand template is G-rich (TG1-3) and forms G4 DNA *in vivo* (31). Furthermore, replication forks stall at human telomeric repeats in yeast whether the TTAGGG repeats are engineered into a plasmid or at chromosome ends (32,33). Circular ssDNA templates were prepared from phagemids containing 10 telomeric repeats inserted in either orientation to generate lagging (G-rich) or leading (C-rich) strand templates (Figure 1A). We previously used these vectors to demonstrate that human telomeric sequence is replicated accurately in normal human cells (28). Oligonucleotide primers allowed for a 3-nt running start (RS) (TCT sequence) before the telomeric sequence. Potential structures that can form within the TTAGGG repeats include G4 DNA and intermediate hairpin or triplex folds (34,35) (Figure 1B). A 1:1 ratio of enzyme to template yielded sufficient progression through the telomeric repeats to detect potential stalling. The time course confirmed the expected multiple hit conditions, whereby the polymerase can rebind and extend previously terminated products during the 30-min reaction (Figure 2) (36). Thus, the bands representing accumulated products reveal prominent sites of polymerase stalling. Pol δ showed a distinct pausing pattern at each G run on the lagging template (pausing at the third G in each repeat Figure 2A and B), but was more processive on the leading template. The strongest pause site on the leading C-rich strand occurred after the telomeric sequences. The Pol δ 3′ to 5′ exonuclease generated some primer degradation products on the G-rich telomeric template; an average of 3.6, 2.5 and 1.7% primer degradation after 5, 15 and 30 min, respectively. Despite the strong pause site at the third and fourth template positions on the nontelomeric template, no primer degradation was detected (Figure 2).

Next we asked whether the replication processivity clamp PCNA would prevent polymerase stalling. RFC protein loads PCNA onto the circular templates. As predicted, PCNA increased the product lengths on all templates (Figure 2). PCNA reduced, but did not eliminate, products of Pol δ pausing on the G-rich template. PCNA also partly suppressed Pol δ primer degradation on the G-rich template, with an average of 3.0, 0.63 and 0.15% primer degradation after 5, 15 and 30 min (Figure 2). The data show DNA synthesis on the G-rich template was a challenge for the PCNA/Pol δ complex.

Mechanism for Pol δ stalling at TTAGGG repeats

To test whether an immediate barrier was responsible for stalling and primer degradation on the G-rich template, we used a primer that allowed for a 6-nt RS before the telomeric sequence (Figure 1, gray primer). When polymerase progression is inhibited, the 3′ primer terminus shuttles from the polymerase active site to the exonuclease active site, resulting in primer degradation (37). Moving the potential barrier further downstream from the start site completely alleviated Pol δ primer degradation,

Figure 1. Templates for DNA synthesis. (**A**) The control, telomeric leading strand or telomeric lagging strand templates were generated by annealing a primer to circular ssDNA. Primers created either a 3- (black line) or 6- (gray line) nt RS before telomeric repeat residues (underlined nucleotides). Sequences of the first 66 template nucleotides are shown 5′ to 3′. (**B**) Schematic of potential secondary structures in TTAGGG repeats. Hairpin and triplex structures are proposed intermediates in G4 folding. Monovalent ions K^+ or Na^+ (gray balls) stabilize the G4.

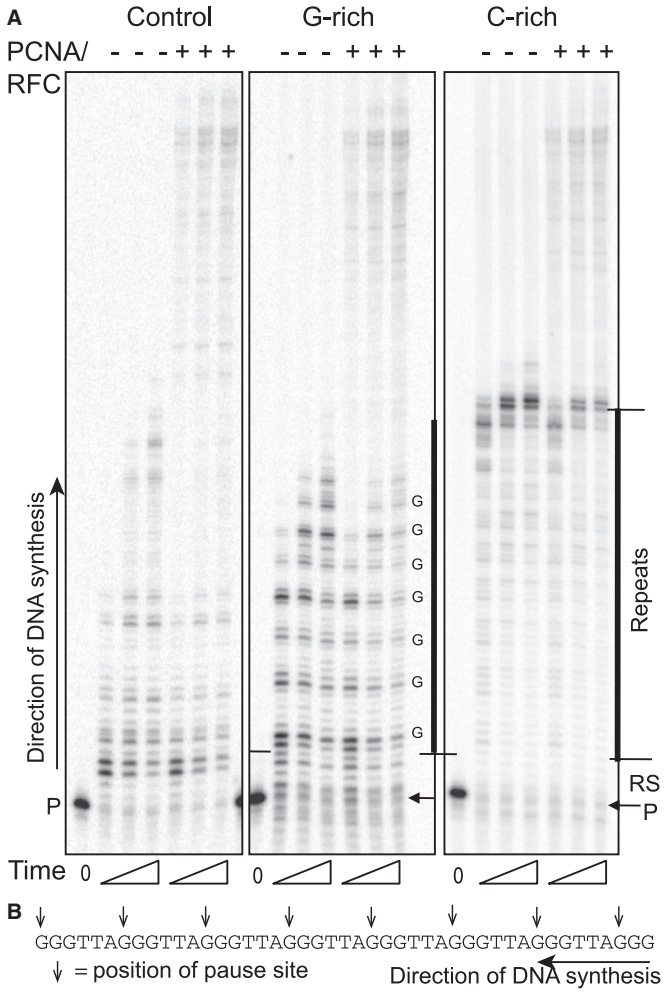

Figure 2. Pol δ stalls at TTAGGG repeats on lagging strand templates. Reactions contained 6.6 nM circular ssDNA primed with a ^{32}P end-labeled 40-mer to allow a 3-nt RS before telomeric sequence (see Figure 1). Reactions were initiated by adding 6.6 nM Pol δ and were incubated under standard conditions and 90 mM NaCl at 30°C. Aliquots were terminated at 5, 15 and 30 min and run on 10% polyacrylamide denaturing gels. (**A**) Gel images for reactions containing Pol δ alone or for templates preincubated with 20 nM PCNA and 13 nM RFC. Thick black lines mark locations of the telomeric repeats, and Gs mark the third guanine of each repeat. RS indicates the 3-nt RS, and P marks the primer. (**B**) Prominent stall sites occurred at the third Gs in the TTAGGG repeats on the template; marked with an arrow.

although stalling at G-runs remained (Supplementary Figure S1).

To determine whether the apparent 'barrier' on the G-rich template is G4 DNA, we repeated the reactions under conditions that suppress or promote G4 formation. Monovalent cations Na^+ or K^+ stabilize a G4 fold by coordinating in the central cavity formed by the guanine tetrads (Figure 1B); however, Li^+ ions are too small for efficient coordination and cannot stabilize the G4 (38). Primers were annealed to templates in either 100 mM KCl or LiCl, and 90 mM NaCl was substituted with either 100 mM KCl or LiCl in the polymerase reactions. Remarkably similar patterns of Pol δ products were observed in both ionic conditions. Surprisingly, substitution with LiCl did not alleviate Pol δ stalling at G-runs or the primer degradation (Figure 3A). The average % primer degradation was 1.9 and 2.7% for K^+ and Li^+, respectively, at 5 min. While reactions under optimal G4 folding conditions (KCl) did not enhance Pol δ stalling, it caused a near 2-fold increase in products terminated within the 3-nt RS before the repeats, compared with LiCl (Figure 3B). This suggests that KCl was promoting some G4 folding that partly impeded polymerase progression.

Previous reports showed that K^+ induces greater G4 stability and DNA polymerase arrest at G4-forming sequences, compared with Na^+ (39,40). Thus, the result that 100 mM KCl does not significantly block Pol δ progression on the $(TTAGGG)_{10}$ templates was surprising. Some evidence suggests that the number of telomeric repeats affects G4 stability, and that molecules with greater repeat numbers are less thermally stable than molecules with four repeats (41). Therefore, we predicted that reducing the repeat number to four would enhance the inhibition of Pol δ progression. Unexpectedly, Pol δ synthesis on the $(TTAGGG)_4$ template was more similar under the different ionic conditions (K^+ versus Li^+), compared with the $(TTAGGG)_{10}$ template (Figure 3C and Supplementary Figure S2A). Furthermore, the percent of products terminated within the RS was lower for the $(TTAGGG)_4$ template, compared with the $(TTAGGG)_{10}$ template (Figure 3B and C). Increasing the RS to 6 nt did not alter the results (Supplementary Figure S2B). Collectively, our data indicate that G4 formation is not required for Pol δ stalling on telomeric lagging strand templates. Consistent with this, neither ssDNA binding protein replication protein A nor telomeric ssDNA binding protein POT1 prevented Pol δ stalling on the TTAGGG templates (data not shown), despite the ability of these proteins to disrupt G4 folds (42–44).

Pol δ inhibition is greater on linear compared with circular (TTAGGG) templates in K^+ buffer

The result that Pol δ progression is not significantly blocked on the $(TTAGGG)_4$ templates is surprising based on the wealth of structural data that shows $(TTAGGG)_4$ ssDNA forms stable G4 structures (14,41,45). However, these studies used linear ssDNA. Therefore, we tested Pol δ DNA synthesis on linear templates containing either 10 or 4 telomeric repeats. PCNA was omitted because it slides off linear templates; therefore, we tested various Pol δ concentrations reacted for 30 min. Substrates were annealed in either 100 mM KCl or LiCl, and included a 6-nt RS. The K^+ buffer inhibited Pol δ progression on both the $(TTAGGG)_{10}$ and $(TTAGGG)_4$ templates, compared with Li^+ (Figure 4, panels 1–2). K^+ increased the percent of products terminated within the RS region by 2-fold on the $(TTAGGG)_{10}$ templates, and by 7-fold on the $(TTAGGG)_4$ templates at the highest Pol δ concentrations. K^+ also increased the percent of degraded primers for both templates [0.53% (Li^+) versus 3.6% (K^+) on the $(TTAGGG)_4$ templates at 6.6 nM Pol δ]. We replaced the middle G with 7-deazaG in the first and third repeats to prevent Hoogsteen bonding and G4 folding (34). This eliminated the K^+-dependent Pol δ inhibition; however, stalling at the G repeats

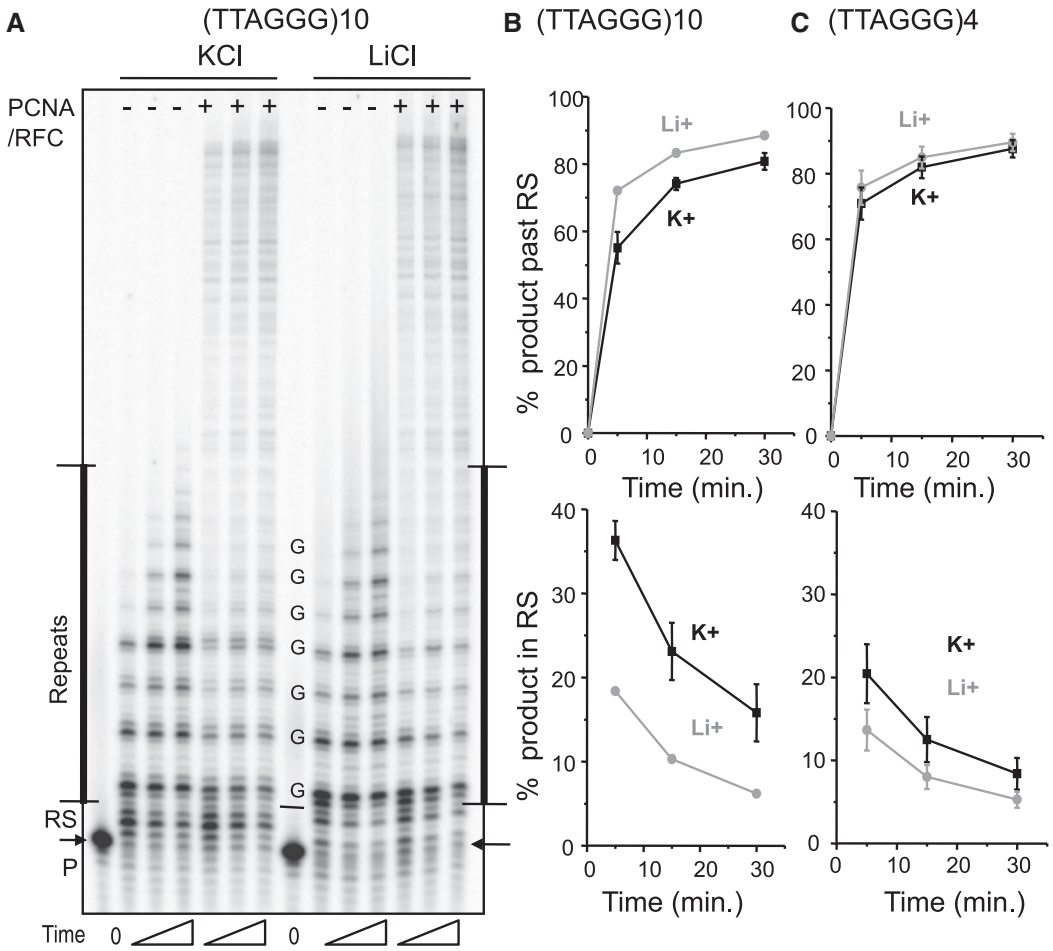

Figure 3. Preventing G4 folding on telomeric lagging strand templates does not suppress Pol δ stalling. Reactions contained 6.6 nM of circular ssDNA templates containing 10 (**A–B**) or 4 (**C** and Supplementary Figure S2) TTAGGG repeats, primed with a 40-mer for a 3-nt RS. Primers were annealed in either 100 mM KCl or 100 mM LiCl. Reactions were initiated by adding 6.6 nM Pol δ alone or with 20 nM PCNA and 13 nM RFC, and were conducted under standard conditions except NaCl was substituted with 100 mM KCl or 100 mM LiCl. Aliquots were terminated at 5, 15 and 30 min and run on denaturing gels. Thick lines mark the telomeric repeats. RS indicates the running start, P marks the primer and Gs indicate the third guanine of each repeat. (B–C) Quantitation of Pol δ/PCNA/RFC reactions on $(TTAGGG)_{10}$ (B) or $(TTAGGG)_4$ (C) templates. The percent of primers extended past the RS were calculated as a function of total DNA. The percent of products terminated within the RS nucleotides were calculated as a function of total DNA. K^+, black line and squares; Li^+, gray line and circles. Mean and standard deviations from two to three independent experiments.

remained (Figure 4, panel 3). Nontelomeric control templates that lacked G4 folding ability confirmed that the different ionic conditions do not alter Pol δ catalysis (Figure 4, panel 4). In summary, increased Pol δ inhibition on the linear templates with four repeats, compared with 10, is consistent with increased G4 folding stability.

The greater K^+-dependent inhibition of Pol δ DNA synthesis on linear compared with circular templates suggests differences in G4 formation. To test whether nucleotides flanking the TTAGGG repeats in the circles could pair with the repeats and prevent G4 formation, we used Mfold to identify potential secondary structures in the polymerase reaction conditions (46). Two thermodynamically favored structures were predicted. One was an interrupted 7-bp hairpin immediately following the repeats, and the other was an interrupted 7-bp hairpin involving the last two repeats of either the $(TTAGGG)_4$ or $(TTAGGG)_{10}$ construct (Supplementary Figure S3). The latter hairpin would prevent G4 folding only in the $(TTAGGG)_4$ circle. To eliminate hairpin formation, we annealed a 39-mer oligonucleotide containing a blocked 3′ terminus to the 5′ flank of the repeats. No synthesis was observed past the resulting 39-bp duplex (Supplementary Figure S4). Using a 6-nt RS primer we observed only a 2-fold difference in products terminated within the RS region for reactions in K^+, compared with Li^+, and no difference after 30 min (Supplementary Figure S4D). Under the identical conditions in K^+, there was significantly more synthesis past the repeats on the circular gaps (Supplementary Figure S4A, lane 4), compared with the linear templates (Figure 4, panel 2, lane 4) (81 ± 4.1% versus 42 ± 4.0%). In contrast, synthesis past the repeats was similar in Li^+ (81.2 ± 1.4% on circular gaps versus 82 ± 3.6 on linear templates) (Figure 4 and Supplementary Figure S4). Thus, interference by flanking nucleotides does not explain why G4 formation appears to present a stronger barrier to polymerase progression on telomeric linear templates compared with circular templates.

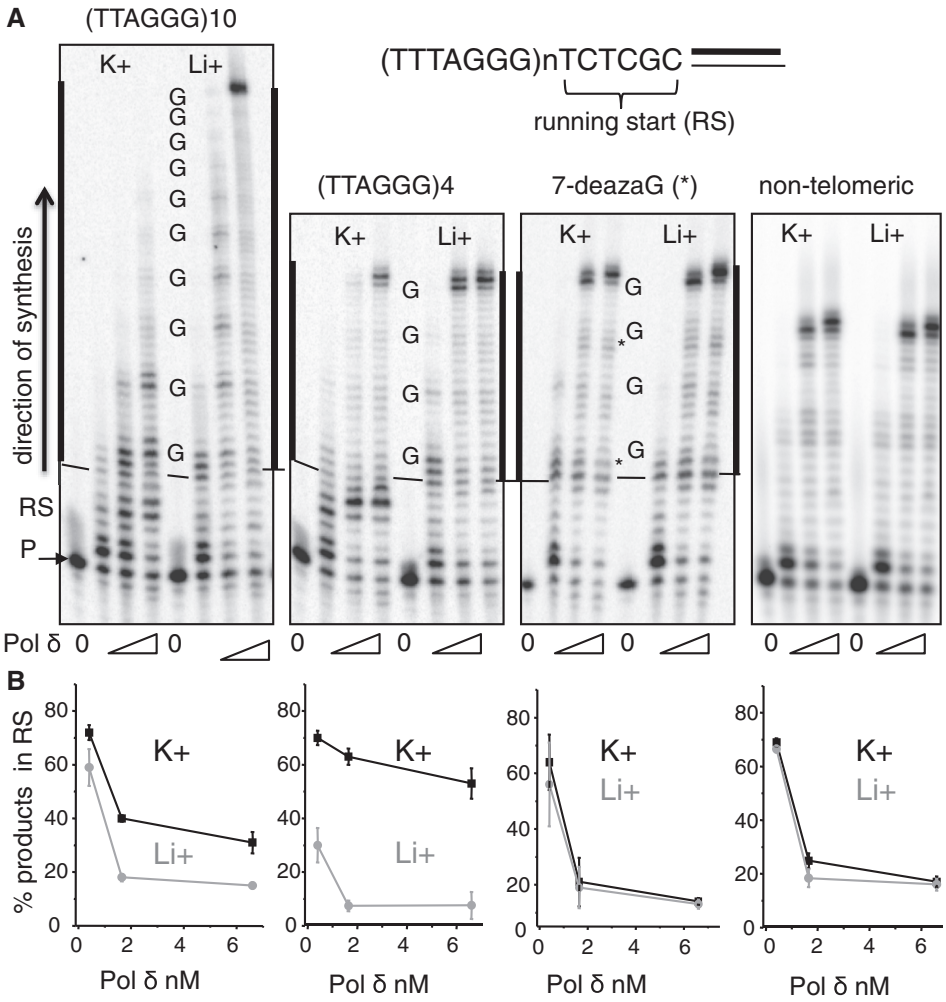

Figure 4. Pol δ exhibits increased blockage on linear templates with 4 TTAGGG repeats compared with 10 in the presence of KCl. (**A**) Reactions contained 6.6 nM linear ssDNA with 10 or 4 (TTAGGG) repeats, four repeats with two 7-deazagaunine substitutions (indicated by asterisk), or a nontelomeric sequence (Supplementary Table S1). Templates were annealed with a primer in either 100 mM KCl or LiCl, for a 6-nt RS (see schematic). Reactions were initiated with 0.41, 1.6 or 6.6 nM Pol δ and were incubated under standard conditions except NaCl was replaced with 100 mM KCl or LiCl. Reactions were terminated at 30 min and run on denaturing gels. Thick lines mark repeats, RS marks the first 6 nt, P indicates primers and Gs mark the third guanine of each repeat. (**B**) The percent of products terminated within the RS was calculated as a function of total DNA. K^+, black line and squares; Li^+, gray line and circles. Mean and standard deviations from two to three independent experiments.

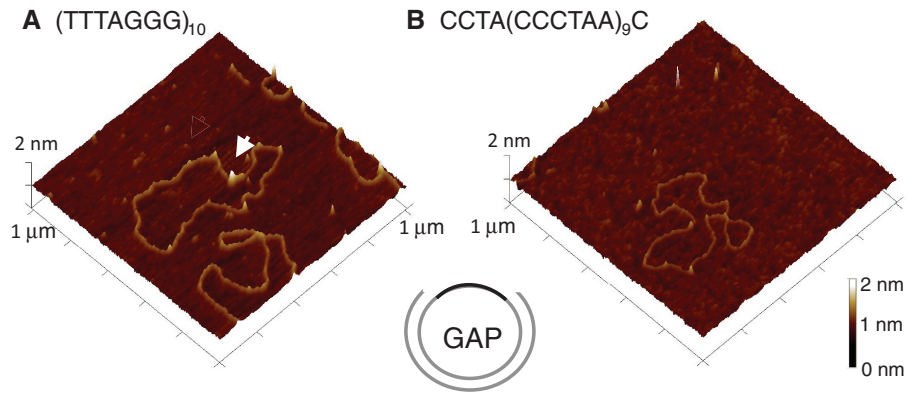

Figure 5. A greater fraction of linear templates exhibit stable G4 structures compared with circular templates. Representative AFM images of circular gapped DNA substrates with $(TTAGGG)_{10}$ ssDNA (**A**) or $CCTAA(CCCTAA)_9C$ ssDNA (**B**) regions. The image is 1 × 1 µm at 2 nm Z-scale. The white arrow points to a characteristic G4 structure (height = 1.2 nm) on a circular $(TTAGGG)_{10}$ gapped substrate.

Another possibility is that the frequency or stability of G4 formation on linear molecules is greater than on circular molecules. To test this we measured the fraction of substrates showing G4 structures by AFM imaging. Different DNA structures, including ssDNA, duplex DNA and G4 folds, can be delineated on AFM images by comparing molecular heights (44,47,48). We established previously that G4 structures in AFM images of oligonucleotides containing TTAGGG repeats exhibit a mean peak height at 0.9 (±0.2) nm (44). To examine the frequency of forming stable higher order DNA structures on circular templates, we prepared duplex plasmids containing an ssDNA gap of 157 nt [$(TTAGGG)_{10}$ sequence flanked by 28 and 69 nt of nontelomeric sequence that cannot form G4]. Imaging of gapped plasmids was required because ssDNA circular plasmids appear condensed, perhaps owing to interactions between complementary sequences (49). A minor population (15%, $N = 34$) of the circular $(TTAGGG)_{10}$ gapped molecules displayed a region with peak heights >0.5 nm (average 1.1 ± 0.2 nm), consistent with the formation of G4 and intermediate structures (Figure 5A) (44). When the G-rich repeats were replaced with (CCCATT) repeats, the gapped plasmids did not display any regions with heights >0.5 nm ($N = 20$) (Figure 5B). AFM images of linear $(TTAGGG)_{10}$ molecules under the identical conditions revealed particles with mean peak heights of 0.79 ± 0.36 nm, consistent with secondary structures and G4 folding (Supplementary Figure S6A and C) (44). Substituting Li^+ for Na^+ yielded molecules with heights at 0.24 ± 0.057 nm, which are less than double-stranded DNA (0.37 ± 0.079 nm) and are consistent with ssDNA (Supplementary Figure S5B and C). In contrast to circular $(TTAGGG)_{10}$ molecules, most of the linear $(TTAGGG)_{10}$ molecules formed secondary structures consistent with G4 or intermediate structures (74%), indicated by heights ranging from 0.5 to 1.63 nm (Supplementary Figure S5C). Thus, a greater fraction of linear molecules with TTAGGG repeats exhibit G4 structures, compared with circular molecules, which corresponds with the increased Pol δ inhibition on linear templates.

Pol δ stalling at G-rich repeats is conserved

Next we asked whether human Pol δ (hPol δ) exhibits similar stalling on the TTAGGG templates, compared with yeast. We used hPol δ and human PCNA amounts that yielded similar levels of total primer extension on the $(TTAGGG)_{10}$ circles compared with yeast after 30 min (95 ± 1.1% for yeast and 94 ± 1.3% for human). Similar to yeast, hPol δ also showed stalling at the third G of each repeat and primer degradation on the lagging strand TTAGGG template (Figure 6). While both enzymes showed improved processivity on the C-rich leading strand, compared with the lagging strand, the human enzyme yielded more prominent stall products on the leading strand corresponding to the third C of each repeat (Figure 6 compared with Figure 2). The reactions were conducted under the established optimal conditions for hPol δ of 5 mM NaCl; however, low monovalent ion concentrations do not support stable G4 folding (29,50).

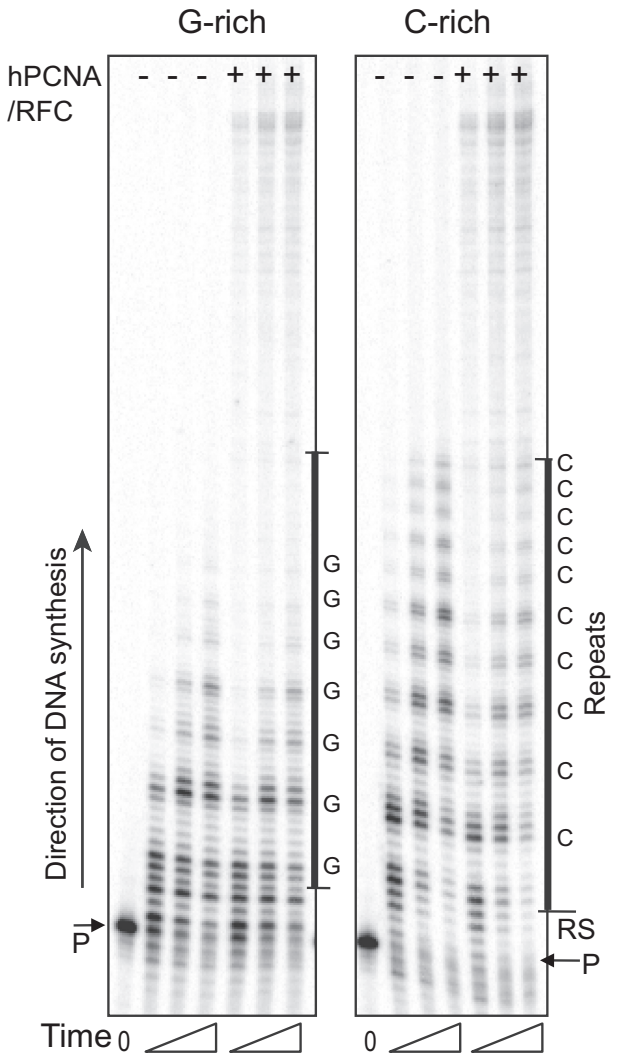

Figure 6. Pol δ stalling within G-rich telomeric repeats is conserved. Reactions contained 6.6 nM ssDNA primed with a 40-mer for a 3-nt RS (see Figure 1). Reactions were initiated by adding 10 nM human Pol δ and were incubated under standard conditions with 5 mM NaCl at 37°C. Aliquots were terminated at 5, 15 and 30 min and run on denaturing gels. Gel images are shown for reactions containing Pol δ alone or for templates preincubated with 170 nM human PCNA and 13 nM RFC as indicated. Thick lines indicate telomeric repeats, P marks the primer, RS indicates the running start and Gs or Cs indicate the third guanine or cytosine, respectively, in each repeat.

We observed that human Pol δ showed greatly reduced activity under high salt, precluding comparisons in 100 mM K^+ versus Li^+ reaction conditions (data not shown).

To modulate G4 folding we added BRACO-19, a well established G4 stabilizing ligand with high affinity for telomeric G4 DNA (51). Reactions were conducted with 30 mM KCl or LiCl for 30 min with increasing BRACO-19 concentrations. Reactions in K^+ showed a slight increase in products terminated within the RS and additional pause sites at TA residues, compared with reactions in Li^+ (Figure 7 compare lanes 2 and 9). The K^+-dependent alterations were greatly enhanced by BRACO-19, which induced a complete shift in pausing at Gs to

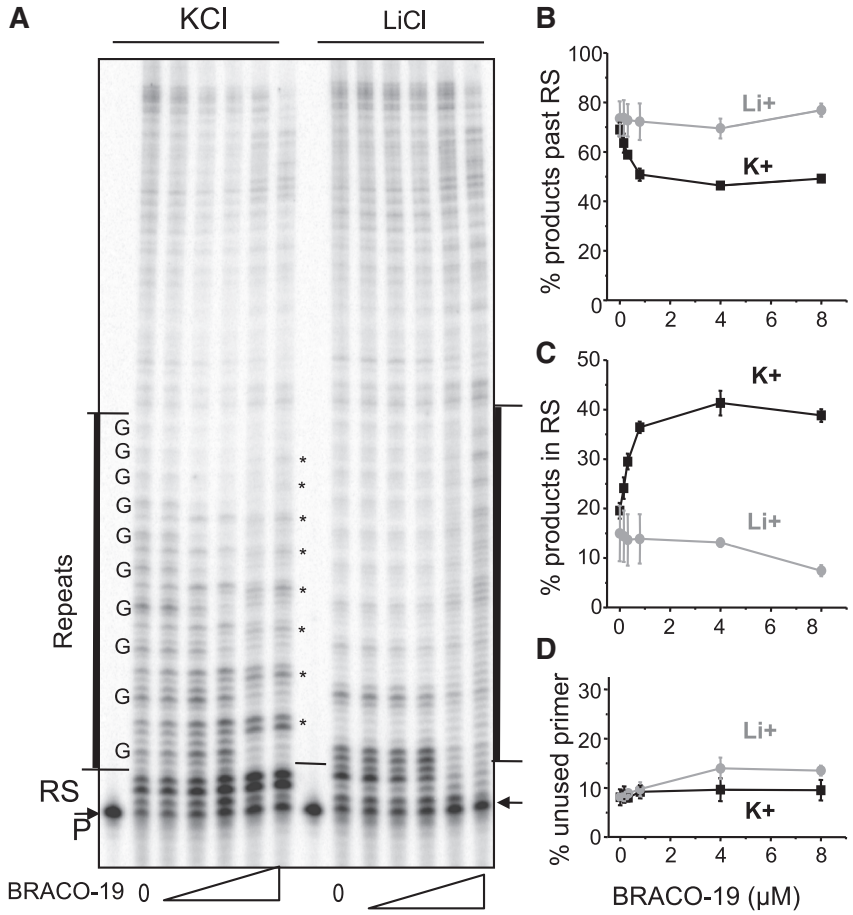

Figure 7. G4 stabilizer BRACO-19 increases Pol δ stalling and blockage on TTAGGG templates in the presence of K^+. (**A**) The $(TTAGGG)_{10}$ circular ssDNA substrate was annealed in either 100 mM KCl or LiCl with a primer for a 3-nt RS. Polymerase reactions contained 6.6 nM templates preincubated with 0, 0.16, 0.32, 0.80, 4.0 or 8.0 μM BRACO-19, 170 nM hPCNA and 13 nM RFC. Reactions were initiated by adding 10 nM hPol δ, and were conducted in standard conditions except NaCl was substituted with either 30 mM KCl or LiCl. Aliquots were terminated at 5, 15 and 30 min and run on denaturing gels. Thick lines indicate telomeric repeats, P marks the primer, RS indicates the running start and Gs indicate the third guanine in each repeat. Asterisk indicates shift to pause sites at TA sites. (B) The percent of primers extended past the RS. (C) The percent of products terminated within the three RS. (**D**) The percent of unextended primers. K^+, black line and squares; Li^+, gray line and circles. Data are mean and standard deviations from two to three independent experiments.

pausing at TA sites, and caused a 5-fold increase in products terminated within the RS at 8 μM BRACO-19. BRACO-19 did not induce these changes in reactions containing Li^+; however, the highest ligand concentrations caused some nonspecific inhibition of total DNA synthesis. Similar results were achieved with yeast Pol δ (Supplementary Figure S6). The results indicate that both G4 folding and G4-independent mechanisms can induce hPol δ stalling on telomeric lagging strand templates.

DISCUSSION

A great deal of evidence from mammalian cells and yeast indicate that telomeres are difficult regions to replicate (23). The G-rich lagging strand is preferentially lost in the absence of some telomeric and DNA repair proteins (9,10). The ability of $(TTAGGG)_4$ sequences to form secondary G4 structures, and the result that G4 folds arrest DNA polymerases *in vitro*, led to the model that quadruplex formation impedes telomere replication (5,9,20). Here we examined for the first time DNA synthesis on telomeric lagging strand templates by the lagging strand replicative polymerase *in vitro*. We observed that Pol δ can proceed through the telomeric TTAGGG repeats, but significant stalling occurs at G-runs within the repeats even in the presence of PCNA processivity factor. Stalling persisted after suppressing G4 formation by altering monovalent ions or by manipulating the template sequence. Our data suggest that telomere fragility and replication fork stalling *in vivo* (5) is due to pausing of the lagging strand replicative DNA polymerase at TTAGGG repeats. However, we provide strong evidence that G4 folds are not required for the apparent stalling, which raises the possibility that G4s are not the main source of telomere replication stalling *in vivo*.

Given the wealth of structural data that shows TTAGGG sequences can spontaneously fold into stable G4s (14,45), the result that Pol δ DNA synthesis is not significantly blocked at the TTAGGG repeats is surprising. Biomolecular G4 folds of the sequence $(CGGG)_7$ present a strong block to yeast Pol δ in 20 mM KCl (18).

In addition, previous studies showed that numerous DNA polymerases arrest on G-rich templates owing to G4 formation in the presence of K^+ or Na^+, but not Li^+ (40). Yet, our results for both yeast and human Pol δ differed. We observed similar extension past the repeats in the presence of K^+ compared with Li^+ on the $(TTAGGG)_{10}$ circular templates (Figures 3 and 7). One likely explanation is that human TTAGGG repeats form less stable G4 folds compared with the G4-forming sequences tested in previous polymerase assays, which primarily used templates with a greater number of Gs in the repeats (39). For example, TTGGGG repeats form more stable G4 folds compared with TTAGGG owing to an additional tetrad of paired G residues (52). Another likely reason is that increasing the number of TTAGGG repeats decreases G4 stability (41), and increases the diversity of G4 conformations and the dynamics of folding and unfolding (H. Hwang, J. Lormand, P. Opresko, and S. Myong, submitted for publication). Consistent with this, we observed greater Pol δ inhibition on the linear templates containing four repeats, compared with 10 repeats (Figure 4). Notably, the nuclear magnetic resonance and crystal structure data were collected from linear molecules with four repeats (45,53). Thus, we expect that G4 folding in the $(TTAGGG)_{10}$ template is highly dynamic and that mobile G4s may allow a polymerase to pass.

The context of TTAGGG repeats influences G4 folding, and thus, also impacts the ability of Pol δ to proceed through the telomeric sequence. We observed that G4 structures are less stable, or fold less frequently, in closed circles compared with linear substrates (Figure 5). This likely explains why preventing G4 folding with Li^+ minimally affected Pol δ progression on the circular templates, but greatly inhibited progression on linear templates (Figures 3 and 4, Supplementary Figure S4). Spatial constraints that exist in the closed circles, but not in the open linear substrates, may influence G4 folding. The ends or borders of the TTAGGG region are constrained within the circles, and how this may influence G4 folding and stability will require future biophysical and structural studies. While negative supercoiling in duplex plasmids was found to generate regions of local unwinding that allow G4 folding, the frequency of G4 folding compared with linear DNA had not been compared (54). The majority of previous work examined G4 stability within linear molecules (14,41). Our data suggest that the spatial constraints that exist within replication bubbles on a chromosome may destabilize G4 folding, and lessen the impact of G4 folding on polymerase progression during telomeric DNA replication.

Because polymerase stalling occurs in the absence of G4 folding, other barriers must impede telomeric lagging strand DNA synthesis. Sequence context effects on DNA synthesis have been demonstrated for various DNA polymerases; however, the molecular mechanisms are not well understood (55). Evidence suggests Pol δ makes extensive contacts with the template ahead of the active site. Structures of yeast Pol δ and related bateriophage polymerase RB69 reveal a channel in the N-terminal domain that is proposed to bind 10–20 nt of the unpaired template strand (56). These contacts with the template may form the basis for the sequence context effects that we observed. Both yeast and human Pol δ exhibit increased slippage errors in $(GT)_{10}$ compared with $(TC)_{11}$ microsatellite sequences (57,58). Human Pol δ-PCNA does not stall at each G on a $(GT)_9$ template, but strongly pauses toward the end of the repeats for unknown reasons (58). Together with our results, this suggests that the topology of some G-rich tracts may be problematic for Pol δ.

Potential barriers in G-rich sequences include intermediates in G4 folding (Figure 1) that do not require K^+ or Na^+. Hairpin and triplex structures can form in TTAGGG repeats through Hoogsteen base pairing between G residues (34,35), and both structures are proposed to impede DNA synthesis in other contexts such as genes responsible for triplet repeat diseases (59). However, stalling at Gs occurred even on the $(TTAGGG)_4$ templates containing two 7-deazaguanine substitutions that prevent Hoogsteen base pairing (Figure 4, panel 3). Single molecule studies revealed that unfolded $(TTAGGG)_4$ molecules are significantly more compact than a polyT construct, possibly owing to increased stacking between purine bases or transient hydrogen bonding (35). We propose that these transient attractive forces lead to stalling at G residues on the TTAGGG template, and that stabilized G4 folds lead to polymerase arrest or stalling at TA residues (Figure 7 and Supplementary Figure S6). This is because G4 stabilization with the BRACO-19 ligand shifts the pause sites from the G runs to the TA residues in the repeats (Figure 7). Structural data indicates that BRACO-19 molecules interact directly with the TA residues when bound to a telomeric G4 (51). Our studies with BRACO-19 reveal both stabilized G4-dependent and independent Pol δ stalling mechanisms on TTAGGG templates.

Our result that yeast Pol δ stalls on telomeric templates is consistent with reports that human telomeric sequences in a plasmid or at chromosome ends induce replication fork stalling in *S. cerevisiae* (32,33). Interestingly, these studies found that RecQ helicase Sgs1 and Pif1 helicase do not prevent replication stalling through human telomeric repeats, although these enzymes unwind G4 DNA *in vitro* and influence replication and transcription in other G4-forming sequence (17,60). Furthermore, mechanical telomeric G4 unfolding studies indicate that only a few base pairs need to be disrupted to destabilize the entire G4 (35). Studies with an antibody that binds G4 structures revealed that the majority of antibody staining occurred outside the telomeres, suggesting that other G-rich sequences in the genome form more stable G4s compared with telomeric sequences (61). These findings further support our conclusion that G4 formation may not be the primary impediment to telomeric lagging strand DNA synthesis, and suggest alternative mechanisms by which specialized helicases may promote telomeric DNA replication in human.

In summary, cellular studies have established telomeric repeats as difficult sequences to replicate in yeast and mammalian cells (23), and our biochemical studies indicate that the lagging strand replicative polymerase stalls on TTAGGG templates. However, our data show

that G4 folding is not required for polymerase stalling during telomeric DNA synthesis, and show that introducing spatial constraints or increasing the number of telomeric repeats reduces G4 stability. This raises the possibility that the specialized DNA helicases WRN, BLM and RTEL may facilitate telomere replication by mechanisms other than unwinding G4 (9,13,22,62). A better understanding of telomeric DNA replication is required to elucidate mechanisms that lead to telomere disruption and loss.

SUPPLEMENTARY DATA

Supplementary Data are available at NAR Online.

ACKNOWLEDGEMENTS

We are grateful to Mercedes Arana and Gregory Sowd for technical support, and to Sua Myong and Helen Hwang for helpful discussion. We thank Walter Chazin (Vanderbilt University) for generously providing recombinant human replication protein A (R01 GM65484).

FUNDING

NIH [R01ES0515052 to P.L.O., R01GM032431 to P.M.B., R00ES016758 to H.W., R01GM031973 to M.Y.L.] (in part); Division of Intramural Research of the National Institutes of Health, NIEHS [Z01 ES065070 to T.A.K.]. Funding for open access charge: Scaife Foundation through the Center for Nucleic Acids Science and Technology at Carnegie Mellon University (to P.L.O.).

Conflict of interest statement. None declared.

REFERENCES

1. Palm,W. and de Lange,T. (2008) How shelterin protects mammalian telomeres. *Annu. Rev. Genet.*, **42**, 301–334.
2. d'Adda di Fagagna,F., Reaper,P.M., Clay-Farrace,L., Fiegler,H., Carr,P., Von Zglinicki,T., Saretzki,G., Carter,N.P. and Jackson,S.P. (2003) A DNA damage checkpoint response in telomere-initiated senescence. *Nature*, **426**, 194–198.
3. Harley,C.B., Futcher,A.B. and Greider,C.W. (1990) Telomeres shorten during ageing of human fibroblasts. *Nature*, **345**, 458–460.
4. Bodnar,A.G., Ouellette,M., Frolkis,M., Holt,S.E., Chiu,C.P., Morin,G.B., Harley,C.B., Shay,J.W., Lichtsteiner,S. and Wright,W.E. (1998) Extension of life-span by introduction of telomerase into normal human cells. *Science*, **279**, 349–352.
5. Sfeir,A., Kosiyatrakul,S.T., Hockemeyer,D., MacRae,S.L., Karlseder,J., Schildkraut,C.L. and de Lange,T. (2009) Mammalian telomeres resemble fragile sites and require TRF1 for efficient replication. *Cell*, **138**, 90–103.
6. Durkin,S.G. and Glover,T.W. (2007) Chromosome fragile sites. *Annu Rev Genet*, **41**, 169–192.
7. Suram,A., Kaplunov,J., Patel,P.L., Ruan,H., Cerutti,A., Boccardi,V., Fumagalli,M., Di Micco,R., Mirani,N., Gurung,R.L. *et al.* (2012) Oncogene-induced telomere dysfunction enforces cellular senescence in human cancer precursor lesions. *EMBO J*, **31**, 2839–2851.
8. Martinez,P., Thanasoula,M., Munoz,P., Liao,C., Tejera,A., McNees,C., Flores,J.M., Fernandez-Capetillo,O., Tarsounas,M. and Blasco,M.A. (2009) Increased telomere fragility and fusions resulting from TRF1 deficiency lead to degenerative pathologies and increased cancer in mice. *Genes Dev*, **23**, 2060–2075.
9. Crabbe,L., Verdun,R.E., Haggblom,C.I. and Karlseder,J. (2004) Defective telomere lagging strand synthesis in cells lacking WRN helicase activity. *Science*, **306**, 1951–1953.
10. Saharia,A., Teasley,D.C., Duxin,J.P., Dao,B., Chiappinelli,K.B. and Stewart,S.A. (2010) FEN1 ensures telomere stability by facilitating replication fork re-initiation. *J Biol Chem*, **285**, 27057–27066.
11. Opresko,P.L., Otterlei,M., Graakjaer,J., Bruheim,P., Dawut,L., Kolvraa,S., May,A., Seidman,M.M. and Bohr,V.A. (2004) The Werner syndrome helicase and exonuclease cooperate to resolve telomeric D loops in a manner regulated by TRF1 and TRF2. *Mol. Cell*, **14**, 763–774.
12. Lillard-Wetherell,K., Machwe,A., Langland,G.T., Combs,K.A., Behbehani,G.K., Schonberg,S.A., German,J., Turchi,J.J., Orren,D.K. and Groden,J. (2004) Association and regulation of the BLM helicase by the telomere proteins TRF1 and TRF2. *Hum. Mol. Genet.*, **13**, 1919–1932.
13. Vannier,J.B., Pavicic-Kaltenbrunner,V., Petalcorin,M.I., Ding,H. and Boulton,S.J. (2012) RTEL1 Dismantles T Loops and Counteracts Telomeric G4-DNA to Maintain Telomere Integrity. *Cell*, **149**, 795–806.
14. Burge,S., Parkinson,G.N., Hazel,P., Todd,A.K. and Neidle,S. (2006) Quadruplex DNA: sequence, topology and structure. *Nucleic Acids Res.*, **34**, 5402–5415.
15. Arnoult,N., Saintome,C., Ourliac-Garnier,I., Riou,J.F. and Londono-Vallejo,A. (2009) Human POT1 is required for efficient telomere C-rich strand replication in the absence of WRN. *Genes Dev.*, **23**, 2915–2924.
16. Mohaghegh,P., Karow,J.K., Brosh,R.M. Jr, Bohr,V.A. and Hickson,I.D. (2001) The Bloom's and Werner's syndrome proteins are DNA structure-specific helicases. *Nucleic Acids Res.*, **29**, 2843–2849.
17. Paeschke,K., Capra,J.A. and Zakian,V.A. (2011) DNA replication through G-quadruplex motifs is promoted by the Saccharomyces cerevisiae Pif1 DNA helicase. *Cell*, **145**, 678–691.
18. Kamath-Loeb,A.S., Loeb,L.A., Johansson,E., Burgers,P.M. and Fry,M. (2001) Interactions between the Werner syndrome helicase and DNA polymerase delta specifically facilitate copying of tetraplex and hairpin structures of the d(CGG)n trinucleotide repeat sequence. *J. Biol. Chem.*, **276**, 16439–16446.
19. Nick McElhinny,S.A., Gordenin,D.A., Stith,C.M., Burgers,P.M. and Kunkel,T.A. (2008) Division of labor at the eukaryotic replication fork. *Mol. Cell*, **30**, 137–144.
20. Lansdorp,P.M. (2005) Major cutbacks at chromosome ends. *Trends Biochem. Sci.*, **30**, 388–395.
21. Verdun,R.E. and Karlseder,J. (2007) Replication and protection of telomeres. *Nature*, **447**, 924–931.
22. Opresko,P.L. (2008) Telomere ResQue and preservation—roles for the Werner syndrome protein and other RecQ helicases. *Mech. Ageing Dev.*, **129**, 79–90.
23. Gilson,E. and Geli,V. (2007) How telomeres are replicated. *Nat. Rev. Mol. Cell Biol.*, **8**, 825–838.
24. Burgers,P.M. and Gerik,K.J. (1998) Structure and processivity of two forms of Saccharomyces cerevisiae DNA polymerase delta. *J. Biol. Chem.*, **273**, 19756–19762.
25. Ayyagari,R., Gomes,X.V., Gordenin,D.A. and Burgers,P.M. (2003) Okazaki fragment maturation in yeast. I. Distribution of functions between FEN1 AND DNA2. *J. Biol. Chem.*, **278**, 1618–1625.
26. Xie,B., Mazloum,N., Liu,L., Rahmeh,A., Li,H. and Lee,M.Y. (2002) Reconstitution and characterization of the human DNA polymerase delta four-subunit holoenzyme. *Biochemistry*, **41**, 13133–13142.
27. Sowd,G., Lei,M. and Opresko,P.L. (2008) Mechanism and substrate specificity of telomeric protein POT1 stimulation of the Werner syndrome helicase. *Nucleic Acids Res.*, **36**, 4242–4256.
28. Damerla,R.R., Knickelbein,K.E., Kepchia,D., Jackson,A., Armitage,B.A., Eckert,K.A. and Opresko,P.L. (2010) Telomeric repeat mutagenicity in human somatic cells is modulated by repeat orientation and G-quadruplex stability. *DNA Repair (Amst.)*, **9**, 1119–1129.
29. Shah,S.N., Opresko,P.L., Meng,X., Lee,M.Y. and Eckert,K.A. (2010) DNA structure and the Werner protein modulate human

DNA polymerase delta-dependent replication dynamics within the common fragile site FRA16D. *Nucleic Acids Res.*, **38**, 1149–1162.
30. Hile,S.E. and Eckert,K.A. (2008) DNA polymerase kappa produces interrupted mutations and displays polar pausing within mononucleotide microsatellite sequences. *Nucleic Acids Res.*, **36**, 688–696.
31. Smith,J.S., Chen,Q., Yatsunyk,L.A., Nicoludis,J.M., Garcia,M.S., Kranaster,R., Balasubramanian,S., Monchaud,D., Teulade-Fichou,M.P., Abramowitz,L. *et al.* (2011) Rudimentary G-quadruplex-based telomere capping in Saccharomyces cerevisiae. *Nat. Struct. Mol. Biol.*, **18**, 478–485.
32. Bah,A., Gilson,E. and Wellinger,R.J. (2011) Telomerase is required to protect chromosomes with vertebrate-type T2AG3 3′ ends in Saccharomyces cerevisiae. *J. Biol. Chem.*, **286**, 27132–27138.
33. Anand,R.P., Shah,K.A., Niu,H., Sung,P., Mirkin,S.M. and Freudenreich,C.H. (2012) Overcoming natural replication barriers: differential helicase requirements. *Nucleic Acids Res.*, **40**, 1091–1105.
34. Mashimo,T., Yagi,H., Sannohe,Y., Rajendran,A. and Sugiyama,H. (2010) Folding pathways of human telomeric type-1 and type-2 G-quadruplex structures. *J. Am. Chem. Soc.*, **132**, 14910–14918.
35. Long,X., Parks,J.W., Bagshaw,C.R. and Stone,M.D. (2013) Mechanical unfolding of human telomere G-quadruplex DNA probed by integrated fluorescence and magnetic tweezers spectroscopy. *Nucleic Acids Res.*, **41**, 2746–2755.
36. Kokoska,R.J., McCulloch,S.D. and Kunkel,T.A. (2003) The efficiency and specificity of apurinic/apyrimidinic site bypass by human DNA polymerase eta and Sulfolobus solfataricus Dpo4. *J. Biol. Chem.*, **278**, 50537–50545.
37. Garg,P., Stith,C.M., Sabouri,N., Johansson,E. and Burgers,P.M. (2004) Idling by DNA polymerase delta maintains a ligatable nick during lagging-strand DNA replication. *Genes Dev.*, **18**, 2764–2773.
38. Lee,J.Y., Yoon,J., Kihm,H.W. and Kim,D.S. (2008) Structural diversity and extreme stability of unimolecular Oxytricha nova telomeric G-quadruplex. *Biochemistry*, **47**, 3389–3396.
39. Weitzmann,M.N., Woodford,K.J. and Usdin,K. (1996) The development and use of a DNA polymerase arrest assay for the evaluation of parameters affecting intrastrand tetraplex formation. *J. Biol. Chem.*, **271**, 20958–20964.
40. Woodford,K.J., Howell,R.M. and Usdin,K. (1994) A novel K(+)-dependent DNA synthesis arrest site in a commonly occurring sequence motif in eukaryotes. *J. Biol. Chem.*, **269**, 27029–27035.
41. Vorlickova,M., Chladkova,J., Kejnovska,I., Fialova,M. and Kypr,J. (2005) Guanine tetraplex topology of human telomere DNA is governed by the number of (TTAGGG) repeats. *Nucleic Acids Res.*, **33**, 5851–5860.
42. Hwang,H., Buncher,N., Opresko,P.L. and Myong,S. (2012) POT1-TPP1 regulates telomeric overhang structural dynamics. *Structure*, **20**, 1872–1880.
43. Salas,T.R., Petruseva,I., Lavrik,O., Bourdoncle,A., Mergny,J.L., Favre,A. and Saintome,C. (2006) Human replication protein A unfolds telomeric G-quadruplexes. *Nucleic Acids Res.*, **34**, 4857–4865.
44. Wang,H., Nora,G.J., Ghodke,H. and Opresko,P.L. (2011) Single molecule studies of physiologically relevant telomeric tails reveal POT1 mechanism for promoting G-quadruplex unfolding. *J. Biol. Chem.*, **286**, 7479–7489.
45. Ambrus,A., Chen,D., Dai,J., Bialis,T., Jones,R.A. and Yang,D. (2006) Human telomeric sequence forms a hybrid-type intramolecular G-quadruplex structure with mixed parallel/antiparallel strands in potassium solution. *Nucleic Acids Res.*, **34**, 2723–2735.
46. Zuker,M. (2003) Mfold web server for nucleic acid folding and hybridization prediction. *Nucleic Acids Res.*, **31**, 3406–3415.
47. Lyubchenko,Y.L. (2004) DNA structure and dynamics: an atomic force microscopy study. *Cell Biochem. Biophys.*, **41**, 75–98.
48. Neaves,K.J., Huppert,J.L., Henderson,R.M. and Edwardson,J.M. (2009) Direct visualization of G-quadruplexes in DNA using atomic force microscopy. *Nucleic Acids Res.*, **37**, 6269–6275.
49. Hamon,L., Pastre,D., Dupaigne,P., Le Breton,C., Le Cam,E. and Pietrement,O. (2007) High-resolution AFM imaging of single-stranded DNA-binding (SSB) protein—DNA complexes. *Nucleic Acids Res.*, **35**, e58.
50. Gray,R.D. and Chaires,J.B. (2008) Kinetics and mechanism of K+- and Na+-induced folding of models of human telomeric DNA into G-quadruplex structures. *Nucleic Acids Res.*, **36**, 4191–4203.
51. Campbell,N.H., Parkinson,G.N., Reszka,A.P. and Neidle,S. (2008) Structural basis of DNA quadruplex recognition by an acridine drug. *J. Am. Chem. Soc.*, **130**, 6722–6724.
52. Lee,J.Y., Okumus,B., Kim,D.S. and Ha,T. (2005) Extreme conformational diversity in human telomeric DNA. *Proc. Natl Acad. Sci. USA*, **102**, 18938–18943.
53. Parkinson,G.N., Lee,M.P. and Neidle,S. (2002) Crystal structure of parallel quadruplexes from human telomeric DNA. *Nature*, **417**, 876–880.
54. Sun,D. and Hurley,L.H. (2009) The importance of negative superhelicity in inducing the formation of G-quadruplex and i-motif structures in the c-Myc promoter: implications for drug targeting and control of gene expression. *J. Med. Chem.*, **52**, 2863–2874.
55. Abbotts,J., Bebenek,K., Kunkel,T.A. and Wilson,S.H. (1993) Mechanism of HIV-1 reverse transcriptase. Termination of processive synthesis on a natural DNA template is influenced by the sequence of the template-primer stem. *J. Biol. Chem.*, **268**, 10312–10323.
56. Swan,M.K., Johnson,R.E., Prakash,L., Prakash,S. and Aggarwal,A.K. (2009) Structural basis of high-fidelity DNA synthesis by yeast DNA polymerase delta. *Nat. Struct. Mol. Biol.*, **16**, 979–986.
57. Abdulovic,A.L., Hile,S.E., Kunkel,T.A. and Eckert,K.A. (2011) The in vitro fidelity of yeast DNA polymerase delta and polymerase epsilon holoenzymes during dinucleotide microsatellite DNA synthesis. *DNA Repair (Amst.)*, **10**, 497–505.
58. Hile,S.E., Wang,X., Lee,M.Y. and Eckert,K.A. (2011) Beyond translesion synthesis: polymerase {kappa} fidelity as a potential determinant of microsatellite stability. *Nucleic Acids Res.*, **40**, 1636–1647.
59. Wang,G. and Vasquez,K.M. (2009) Models for chromosomal replication-independent non-B DNA structure-induced genetic instability. *Mol. Carcinog.*, **48**, 286–298.
60. Hershman,S.G., Chen,Q., Lee,J.Y., Kozak,M.L., Yue,P., Wang,L.S. and Johnson,F.B. (2008) Genomic distribution and functional analyses of potential G-quadruplex-forming sequences in Saccharomyces cerevisiae. *Nucleic Acids Res.*, **36**, 144–156.
61. Biffi,G., Tannahill,D., McCafferty,J. and Balasubramanian,S. (2013) Quantitative visualization of DNA G-quadruplex structures in human cells. *Nat. Chem.*, **5**, 182–186.
62. Barefield,C. and Karlseder,J. (2012) The BLM helicase contributes to telomere maintenance through processing of late-replicating intermediate structures. *Nucleic Acids Res.*, **40**, 7358–7367.